Puzzles of Heavy Baryons

Mikhail Mikhasenko

ORIGINS Excellence Cluster, Munich

April 21st, 2023

Exotic Hadron Spectroscopy

Why studying charm hadrons?

- Two types of exotics:
  - Genuine exotics – no convent. expected
  - **Mixture** – the conventional states are influenced particle interaction.
    Mass shift towards the strongly-coupled threshold.
- b/c hadrons are narrow
- Level-splitting hierarchy due to $1/m_Q$

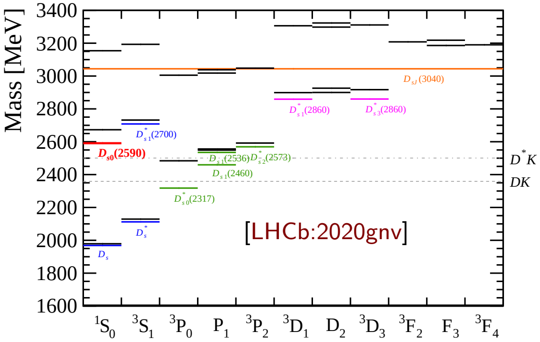

Why studying charm hadrons?

- Two types of exotics:
  - Genuine exotics – no convent. expected
  - **Mixture** – the conventional states are influenced particle interaction.
    Mass shift towards the strongly-coupled threshold.
- b/c hadrons are narrow
- Level-splitting hierarchy due to $1/m_Q$

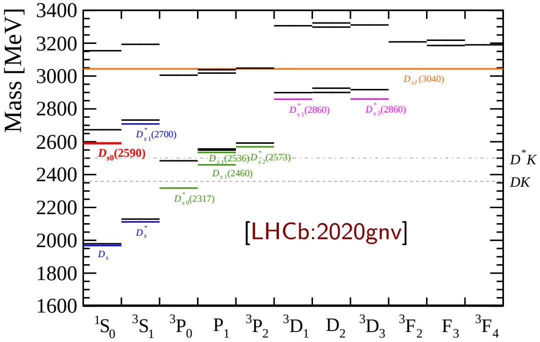

Baryons

- Quark-diquark picture
- Many deeply connected sectors, e.g.

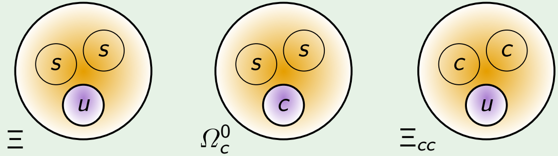

Lattice QCD: 5 λ modes and 2 ρ modes

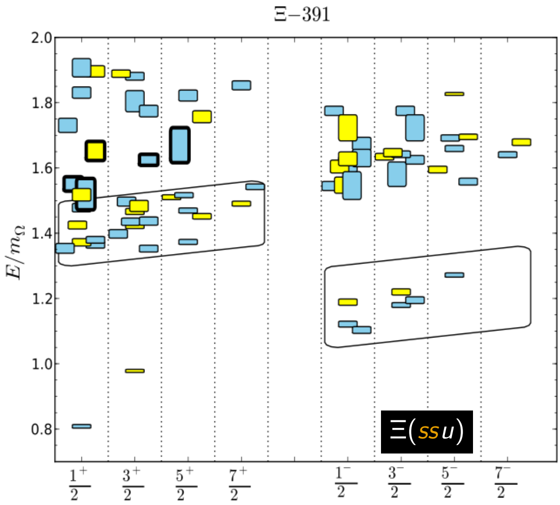

[PRD87 (2013) 054506]

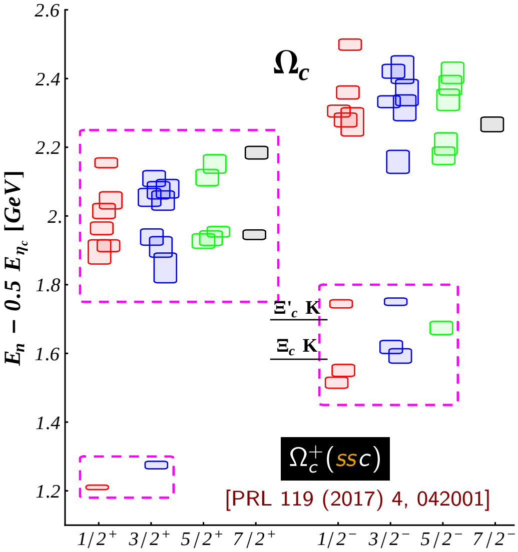

[PRL 119 (2017) 4, 042001]

Heavy-quark-diquark system

Charm-baryon sectors

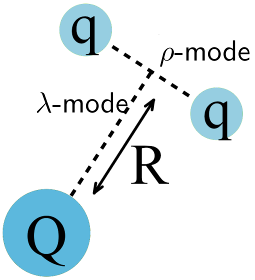

- Heavy quark is **static** and **spinless** in the limit $m_Q \to \infty$.
- Excitations of Qqq are governed by the light diquark
- $q\uparrow^{(J^P=\frac{1}{2}^+)} \otimes q\uparrow^{(J^P=\frac{1}{2}^+)} \quad \Rightarrow \quad \underbrace{\uparrow\downarrow^{(J^P=0^+)}}_{\text{“good”}}$ and $\underbrace{\uparrow\uparrow^{(J^P=1^+)}}_{\text{“bad”}}$
- Excitation pattern is different for “good” and “bad” diquarks

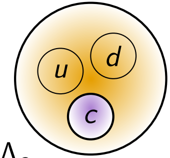

Λ_c

“good”

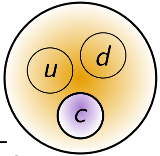

Σ_c

“bad” (isospin)

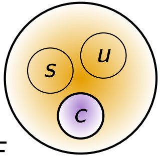

Ξ_c

“good”+“bad”

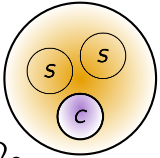

Ω_c

“bad”(identity)

Excitation spectrum of baryons with “bad” diquark

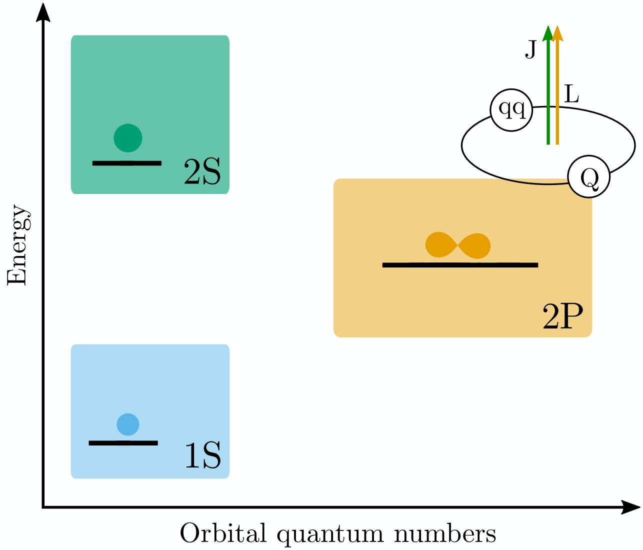

Structure:

- Radial and orbital excitations

Excitation spectrum of baryons with “bad” diquark

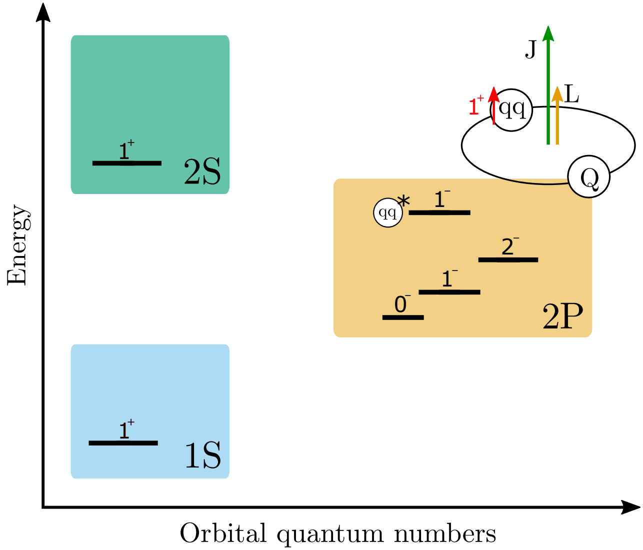

Structure:

- Radial and orbital excitations
- Light d.o.f.: Spin-Orbit splitting

Excitation spectrum of baryons with "bad" diquark

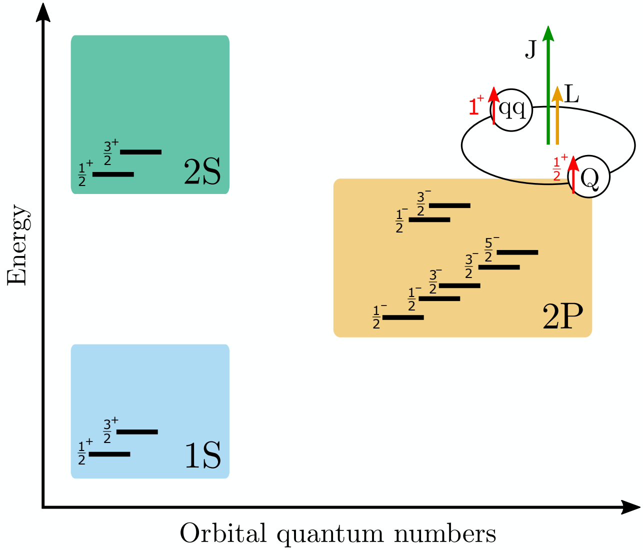

Structure:

- Radial and orbital excitations
- Light d.o.f.: Spin-Orbit splitting
- "Hyperfine" doublets: heavy-quark spin

Excitation spectrum of baryons with “bad” diquark

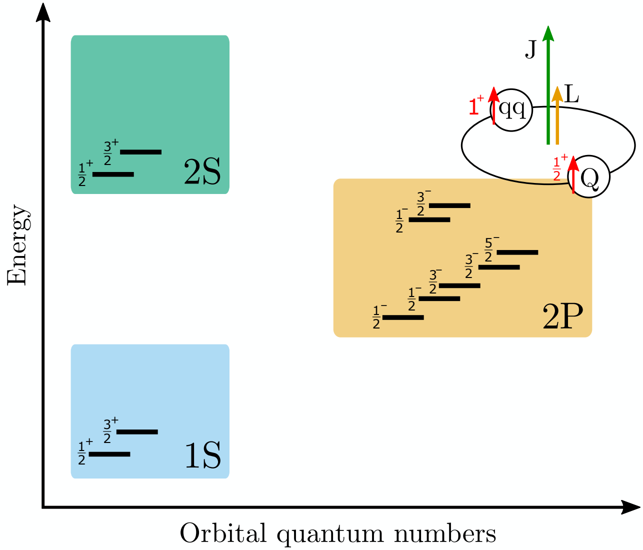

Structure:

- Radial and orbital excitations
- Light d.o.f.: Spin-Orbit splitting
- “Hyperfine” doublets: heavy-quark spin

Counting of states
– model independent
Size of splitting, the order
– differs from model to model

Phenomenological models

- Agree on the general pattern
- Agree on relation between the sectors

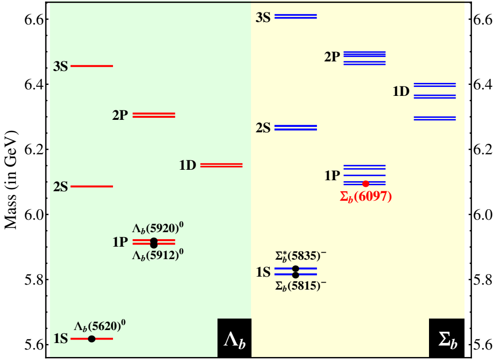

[Bing Chen et al., PRD98 (2018) 074032]

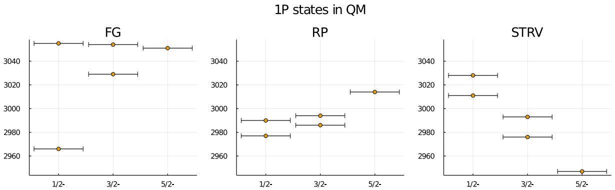

[**F**austov-**G**alkin, EPJ Web Conf. 204 (2019) 08001]
[**R**oberts-**P**ervin, Int.J.Mod.Phys.A 23 (2008) 2817-2860]
[**S**hah-**T**hakkar-**R**ai-**V**inodkumar, EPJA 52 (2016) 10, 313]

- Often neglect the diquark excitation
- Disagree on the splitting and the order

Phenomenological models

- Agree on the general pattern
- Agree on relation between the sectors

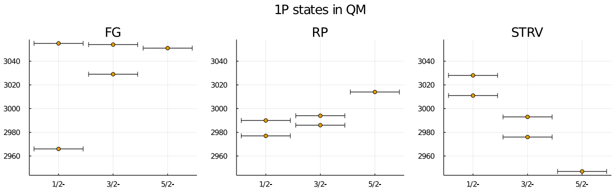

[Faustov-Galkin, EPJ Web Conf. 204 (2019) 08001]
[Roberts-Pervin, Int.J.Mod.Phys.A 23 (2008) 2817-2860]
[Shah-Thakkar-Rai-Vinodkumar, EPJA 52 (2016) 10, 313]

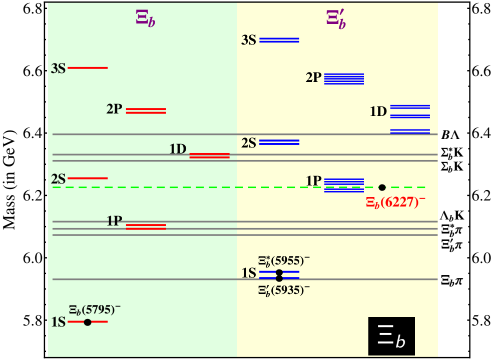

[Bing Chen et al., PRD98 (2018) 031502]

- Often neglect the diquark excitation
- Disagree on the splitting and the order

Strong transitions to a baryon and a pseudoscalar

$$\Omega_c^{**0} \to \Xi_c^+ K^- \qquad \Xi_c^{**0} \to \Lambda_c^+ K^- \qquad \Sigma_c^{**0} \to \Lambda_c^+ \pi^-$$

$$\Omega_b^{**-} \to \Xi_b^0 K^- \qquad \Xi_b^{**-} \to \Lambda_b^0 K^- \qquad \Sigma_b^{**-} \to \Lambda_b^0 \pi^-$$

HQSS ($m_Q \to \infty$) gives the selection rule based on the light d.o.f. [Chiladze, Falk, PRD 56 (1997)]
Can be applied to the decay to ground-state baryon and pseudoscalar ($B + P$):

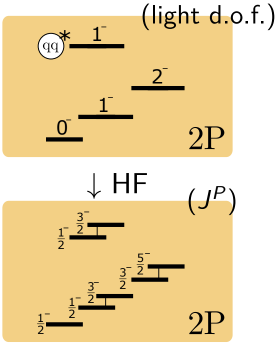

J^P (light d.o.f.)	J^P	$B+P$ (light d.o.f.)	$B+P$
0^-	$1/2^-$	S-wave	S-wave
1^-	$1/2^-$	forbidden	S-wave
	$3/2^-$	forbidden	D-wave
2^-	$3/2^-$	D-wave	D-wave
	$5/2^-$	D-wave	D-wave
1^-	$1/2^-$	forbidden	S-wave
	$3/2^-$	forbidden	S-wave

Four of seven are expected to be suppressed

Experimental results

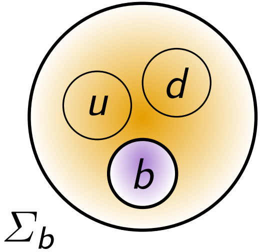
u
d
b
Σ_b

$\Sigma_b^{**\pm}$ states in prompt production [LHCb:2018haf]

Λ_b^0 is reconstructed in $\Lambda_c^+\pi^-$

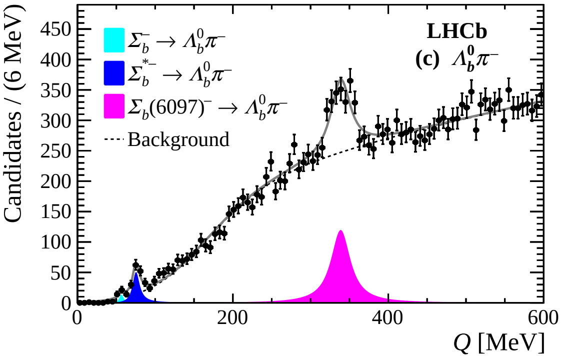

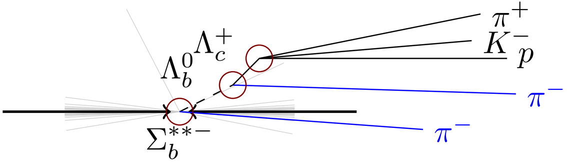

- One clear structure but anomalously broad

$\Sigma_b^{**\pm}$ states in prompt production [LHCb:2018haf]

Λ_b^0 is reconstructed in $\Lambda_c^+\pi^-$

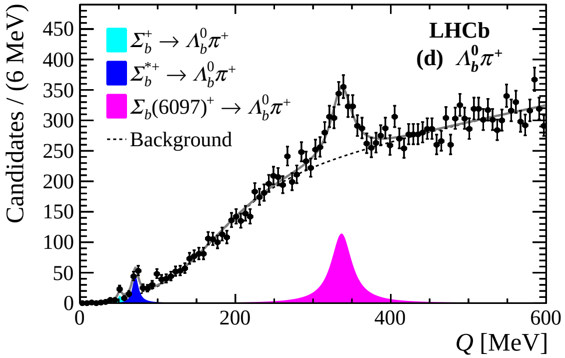

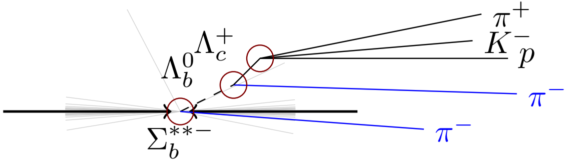

- One clear structure but anomalously broad

$\Sigma_b^{**\pm}$ states in prompt production [LHCb:2018haf]

Λ_b^0 is reconstructed in $\Lambda_c^+\pi^-$

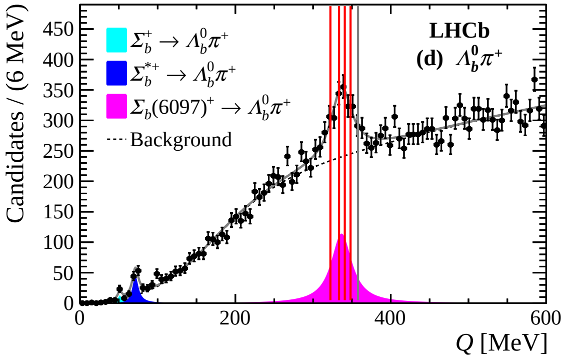

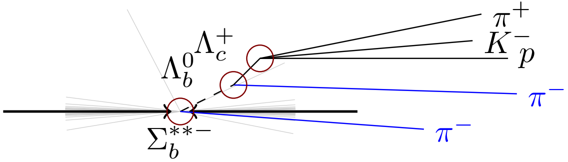

- One clear structure but anomalously broad
- Splitting from Ω_b^{**-} indicates that it will be difficult to resolve.

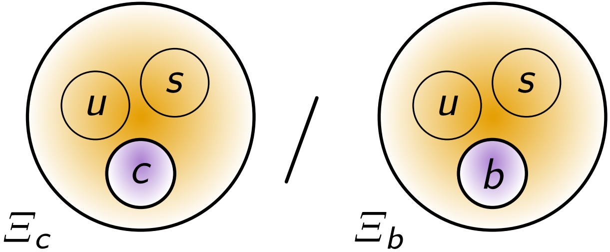
u
s
c
Ξc
/
u
s
b
Ξb

Ξ_c^{**0} states in prompt production

[LHCb, PRL 124, 222001 (2020)]

$$\Xi_c^{**0} \begin{pmatrix} c \\ s \\ d \end{pmatrix} \to \Lambda_c^+ \begin{pmatrix} c \\ u \\ d \end{pmatrix} + K^- \begin{pmatrix} s \\ \bar{u} \end{pmatrix}$$

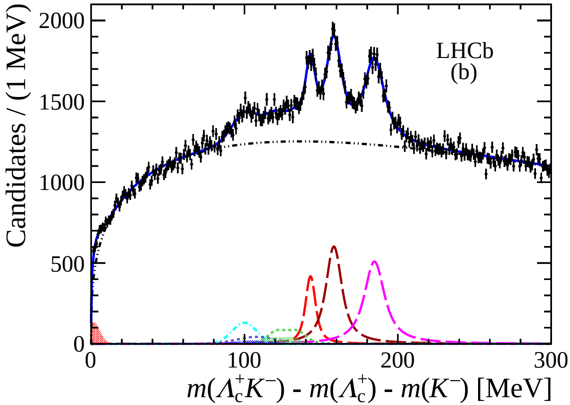

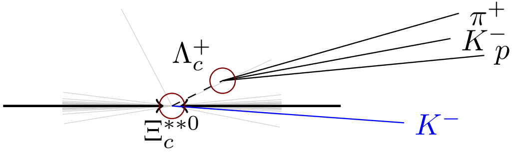

- Four structures are clearly visible
- More cumbersome partially-reconstructed decays
- No fifth narrow state
- The peaks are wider(!)

Ξ_c^{**0} states in prompt production

[LHCb, PRL 124, 222001 (2020)]

$$\Xi_c^{**0} \begin{pmatrix} c \\ s \\ d \end{pmatrix} \to \Lambda_c^+ \begin{pmatrix} c \\ u \\ d \end{pmatrix} + K^- \begin{pmatrix} s \\ \bar{u} \end{pmatrix}$$

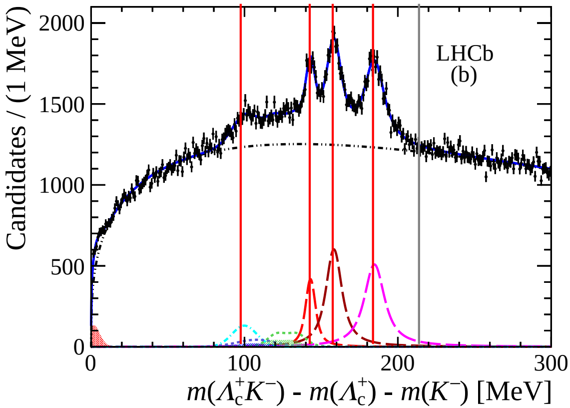

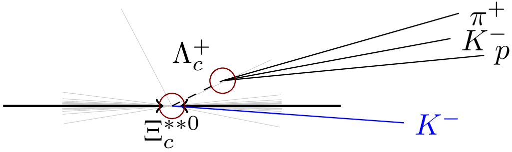

- Four structures are clearly visible
- More cumbersome partially-reconstructed decays
- No fifth narrow state
- The peaks are wider(!)
- Same peak spacing as for Ω_c^{**0}

Ξ_c^{**} states in B decays

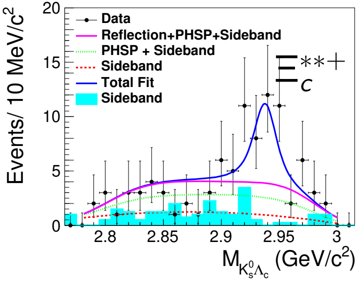

- from e^+e^- machine [Belle:2017jrt]
- Ξ_c^{**0} structures in B decay

$$B^0 \to \Lambda_c^+ \bar{\Lambda}_c^- K^0$$

Ξ_c^{**} states in B decays

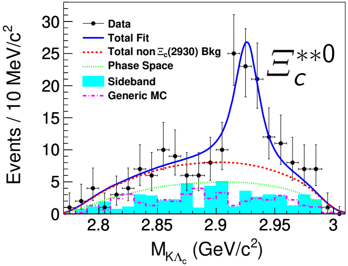

- from e^+e^- machine [Belle:2017jrt]
- Ξ_c^{**0} structures in B decay

$$B^+ \to \Lambda_c^+ \bar{\Lambda}_c^- K^+$$

Ξ_c^{**} states in B decays

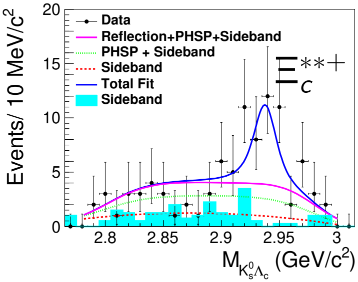

- from e^+e^- machine [Belle:2017jrt]
- Ξ_c^{**0} structures in B decay

$$B^0 \to \Lambda_c^+ \bar{\Lambda}_c^- K^0$$

- in pp collisions [LHCb:2022vns]
- Two dominant states:
  - $\Xi_c(2923)^0$ with $\Gamma = 4.8 \pm 0.9 \pm 1.5\,\text{MeV}$
  - $\Xi_c(2939)^0$ with $\Gamma = 11.0 \pm 1.9 \pm 7.5\,\text{MeV}$
- want to interfere (both $3/2^-$?)

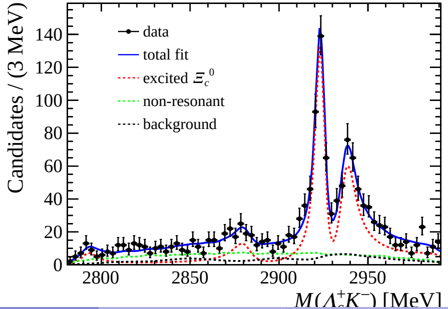

Ξ_b^{**-} states in prompt production

[LHCb, PRD 103, 012004 (2021)]

Λ_b^0 is reconstructed in two final states: $\Lambda_c^+\pi^-$ and $\Lambda_c^+\pi^+\pi^-\pi^-$

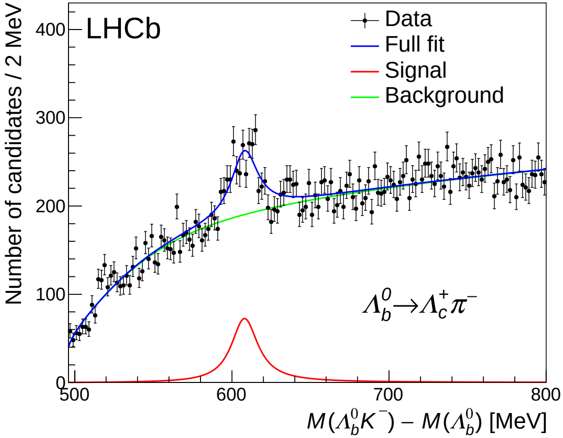

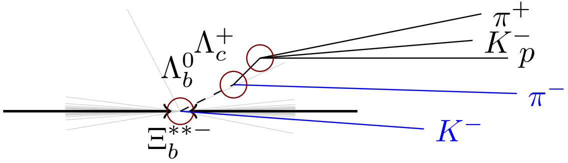

- One clear structure but anomalously broad

Ξ_b^{**-} states in prompt production

[LHCb, PRD 103, 012004 (2021)]

Λ_b^0 is reconstructed in two final states: $\Lambda_c^+\pi^-$ and $\Lambda_c^+\pi^+\pi^-\pi^-$

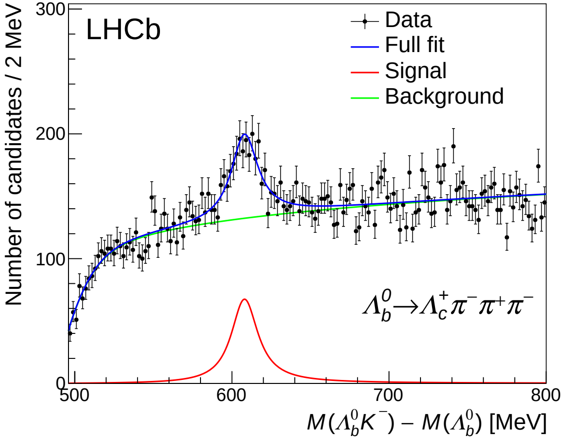

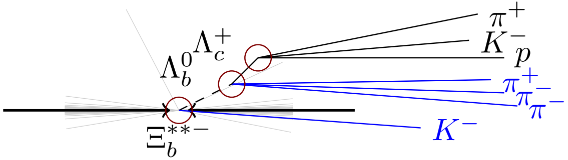

- One clear structure but anomalously broad

Ξ_b^{**-} states in prompt production

[LHCb, PRD 103, 012004 (2021)]

Λ_b^0 is reconstructed in two final states: $\Lambda_c^+\pi^-$ and $\Lambda_c^+\pi^+\pi^-\pi^-$

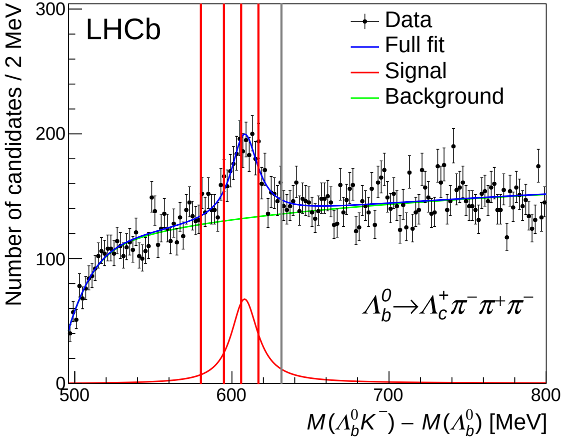

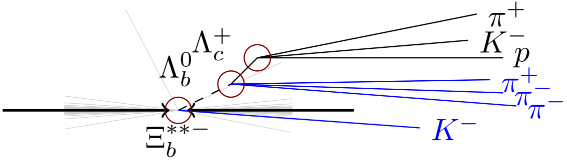

- One clear structure but anomalously broad
- Splitting from Ω_b^{**-} indicates that it will be hard to resolve.

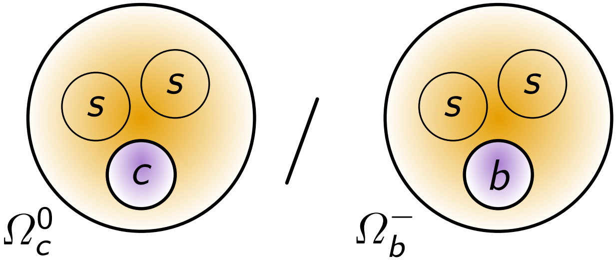
s
s
c
Ω_c^0
/
s
s
b
Ω_b^-

Ω_c^{**0} states in prompt hadroproduction [LHCb:2017uwr]

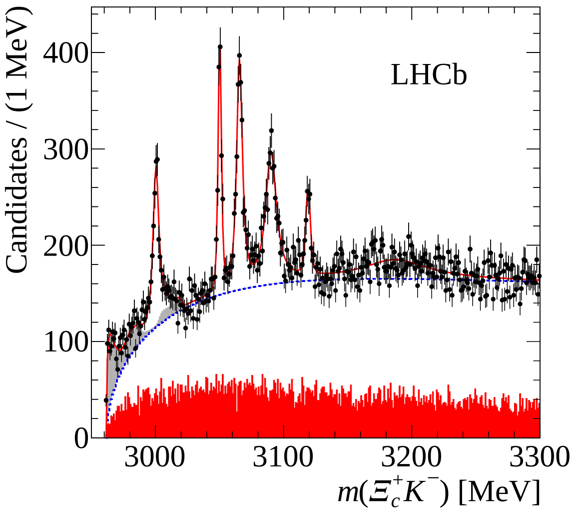

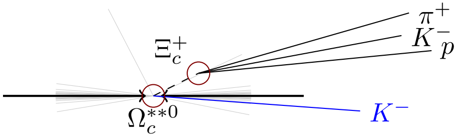

- 5 super-narrow structures
- 1 broad structure
- 3 gray components partially reconstructed $\Omega_c^{**0} \to \Xi_c'^+ (\to \Xi_c^+ \gamma) K$

A popular J^P assignment:
the narrow states are λ modes
in the natural order $\frac{1}{2}^-, \frac{1}{2}^-, \frac{3}{2}^-, \frac{3}{2}^-, \frac{5}{2}^-$.
[Karliner:2017kfm, Padmanath:2017lng, Wang:2017zjw]

Ω_c^{**0} states in prompt electoproduction [Belle:2017ext]

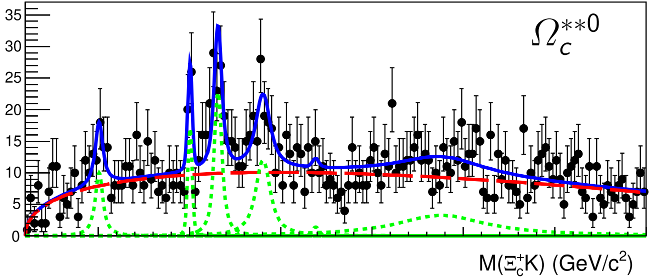

- four Ω_c^{**0} structures are observed in prompt

$$e^+e^- \to \Omega_c^{**0}(\to \Xi_c^+ K^-)\, X$$

Ω_b^{**-} states in prompt production [LHCb:2020tqd]

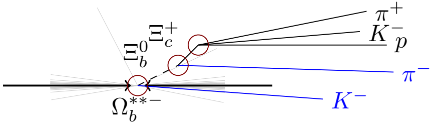

- $\sim$ 100x smaller statistics
- Four peaks are seen with significance $> 3\sigma$
- No fifth narrow state
- Do we see HQSS suppression for the first two?

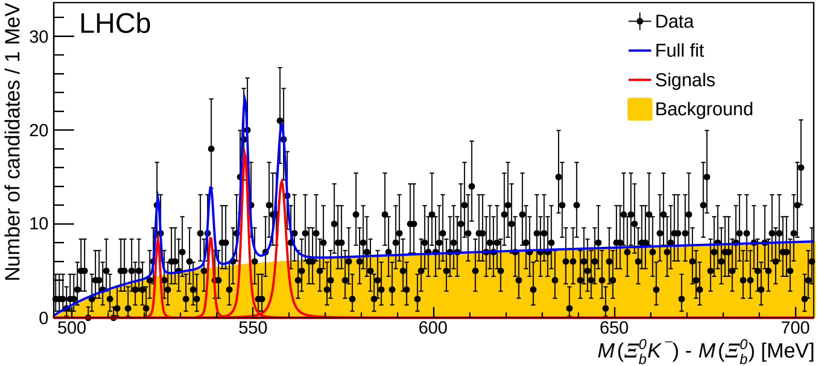

The new states are

$\Omega_b(6315)^-$
$\Omega_b(6330)^-$
$\Omega_b(6340)^-$
$\Omega_b(6350)^-$

The first exclusive observation of Ω_c^{**0} [LHCb:2021ptx]

In $\Omega_b^- \to \Xi_c^+ K^- \pi^-$ decay

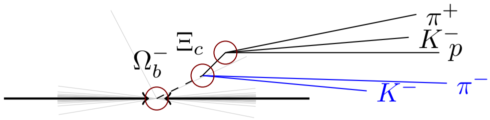

- Strict exclusivity cut $\Rightarrow$ No feed down!
- Same four peaks (no clear fifth)
- $+$ **the threshold structure** (5.3σ)

The first exclusive observation of Ω_c^{**0} [LHCb:2021ptx]

In $\Omega_b^- \to \Xi_c^+ K^- \pi^-$ decay

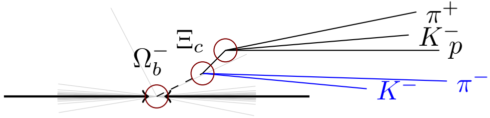

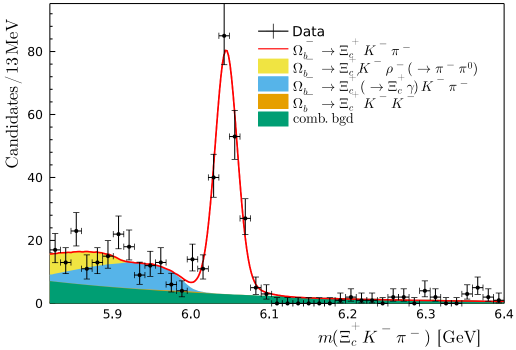

- Strict exclusivity cut $\Rightarrow$ No feed down!
- Same four peaks (no clear fifth)
- $+$ **the threshold structure** (5.3σ)

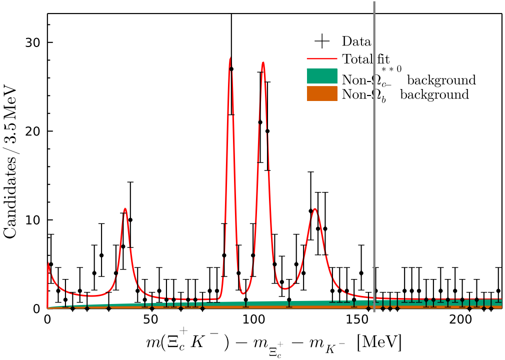

Angular analysis of $\Omega_b^- \to \Omega_c^{**0}(\to \Xi_c^+ K^-)\pi^-$

[LHCb:2021ptx]

- Ω_b^-, Ξ_c spin orientation are averaged
- Still spin sensitivity
  - Spin of Ω_b^- is $1/2$
  - Ω_c^{**0} cannot have spin projection $> 1/2$
  - $\Rightarrow$ non-trivial angular dependence for $J = 3/2$, $J = 5/2$.
  - No parity separation
- Noticeable inefficiency at $\cos\theta = 1$ (soft K^-).

$$3.6\sigma\colon\ J(\Omega_c(3065)^0)\,! = 1/2$$
$$2.2\sigma\colon\ J(\Omega_c(3050)^0)\,! = 1/2$$

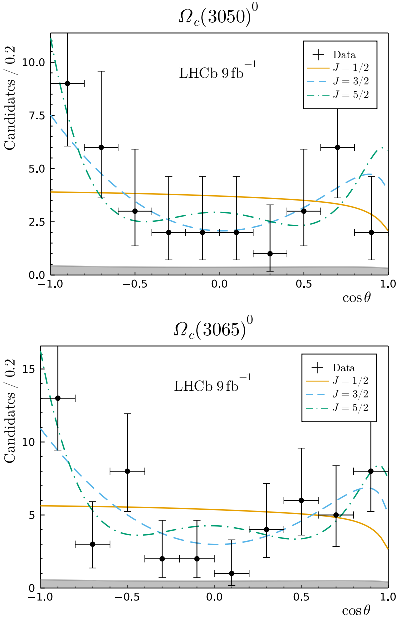

Combined spin test [LHCb:2021ptx]

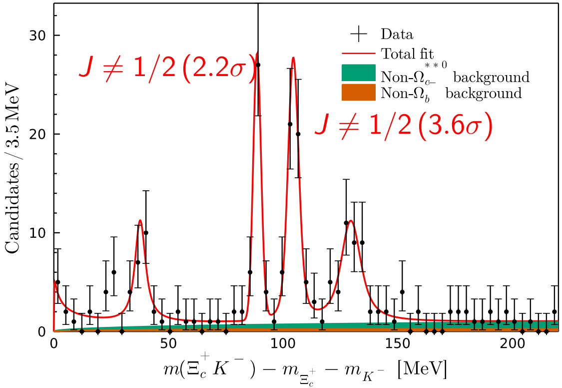

Combined spin test [LHCb:2021ptx]

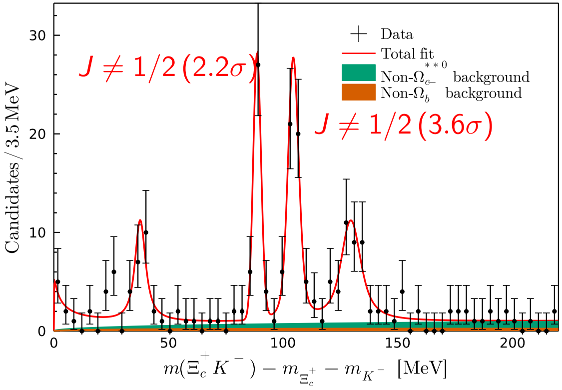

Excluded by 3.6σ

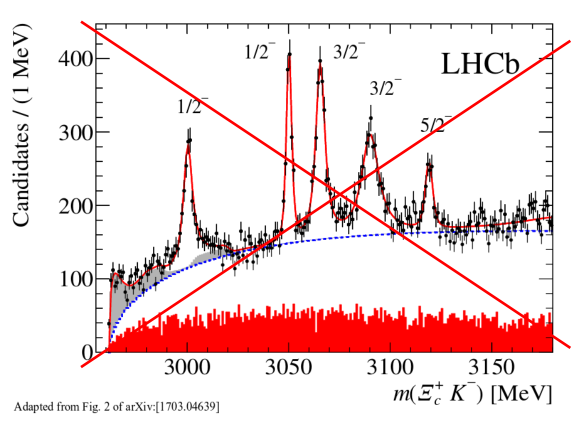

to be revisited!

Combined spin test [LHCb:2021ptx]

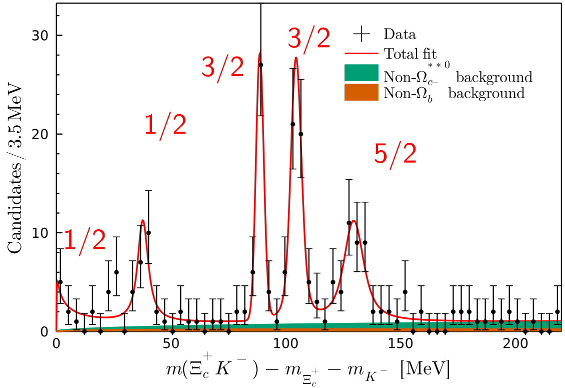

One plausible assignments

Excluded by 3.6σ

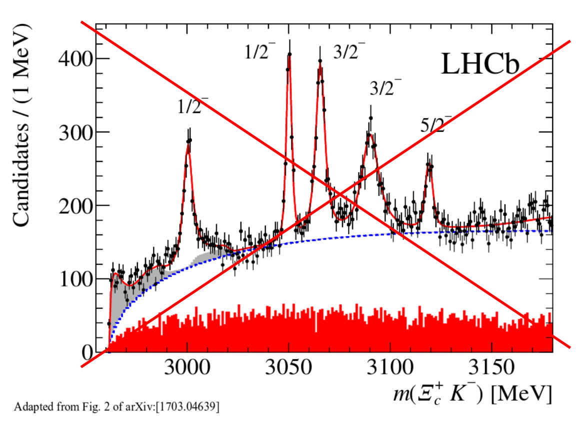

to be revisited!

The threshold structure [LHCb:2021ptx]

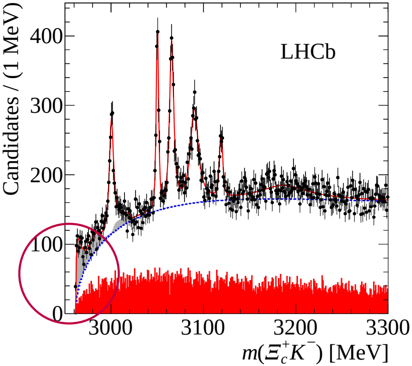

- Explained in the prompt analysis by the partially reconstructed $\Omega_c(3065)^+ \to \Xi_c'^+ K^-$ with anomalously large coupling.

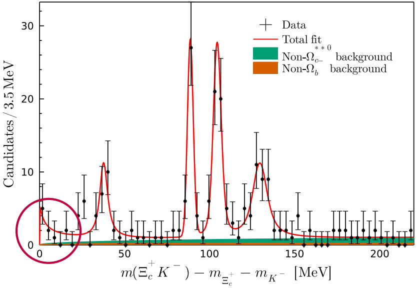

- Exclusive analysis: no feed down is possible
- Other non-physical sources are excluded
- Significance in the nominal fit is 5.3σ, 4.3σ including systematics
- No model sensitivity due to the low statistics

Further investigation in needed!

Further Ω_c^{**0} states from prompt production [LHCb:2023rtu]

- Confirmation of 5-peak structure
- Prominent threshold enhancement
- Two new structures:
  - $\Omega_c(3185)^0$ with $\Gamma = 50 \pm 7^{+10}_{-20}$
  - $\Omega_c(3327)^0$ with $\Gamma = 20 \pm 5^{+13}_{-1}$
- Possibly 2S states [Karliner:2023okv]

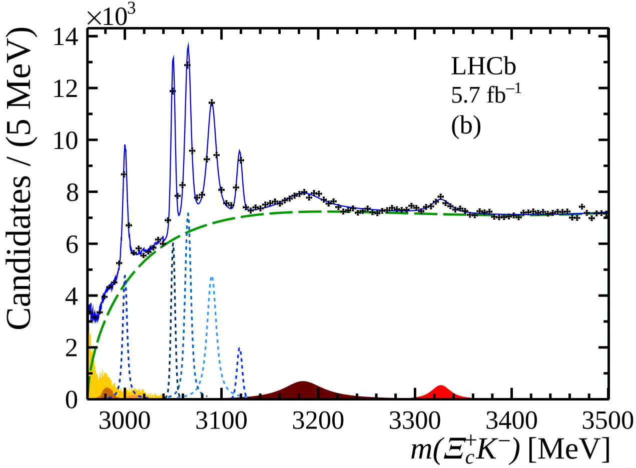

Polarimetry

Weak decay of a fermion deflects reflects polarization

Example: $\Lambda \to p\pi^-$

$$H_{\lambda_\Lambda,\lambda_p} = \langle p, \lambda_p; \pi^- | T_{\text{weak}} | \Lambda, \lambda_\Lambda \rangle$$

$$\frac{2}{\Gamma}\frac{\mathrm{d}\Gamma}{\mathrm{d}\cos\theta} = 1 + P\alpha\cos\theta\,, \quad A_{FB} = \alpha P$$

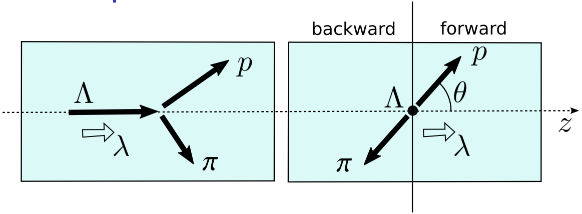

- $P = |\vec{P}|$ polarization, for $J = 1/2$, there are just tree d.o.f.
- α is the **asymmetry parameter**:

Appears only when both PV and PC

$$\alpha = \frac{|H_+|^2 - |H_-|^2}{|H_+|^2 + |H_-|^2} = -\frac{2\mathrm{Re}(H_S{}^* H_P)}{|H_S|^2 + |H_P|^2}$$

S-wave – parity violating (PV); P-wave – parity conserving (PC):

$$\Lambda\,(j^P = 1/2^+) \to p\,(j^P = 1/2^+)\,\pi^-(j^P = 0^-)$$

Weak decay of a fermion deflects reflects polarization

Example: $\Lambda \to p\pi^-$

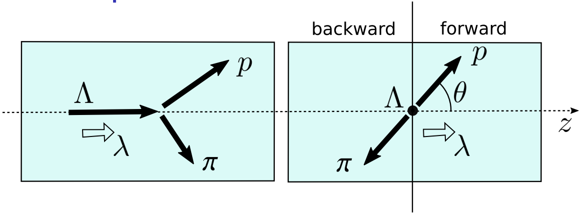

$$H_{\lambda_\Lambda,\lambda_p} = \langle p, \lambda_p; \pi^- | T_{\text{weak}} | \Lambda, \lambda_\Lambda \rangle$$

$$\frac{2}{\Gamma} \frac{\mathrm{d}\Gamma}{\mathrm{d}\cos\theta} = 1 + P\alpha \cos\theta\,, \quad A_{FB} = \alpha P$$

- $P = |\vec{P}|$ polarization, for $J = 1/2$, there are just tree d.o.f.
- α is the **asymmetry parameter**: If we know α, we can measure P

Appears only when both PV and PC

$$\alpha = \frac{|H_+|^2 - |H_-|^2}{|H_+|^2 + |H_-|^2} = -\frac{2\mathrm{Re}(H_S{}^* H_P)}{|H_S|^2 + |H_P|^2}$$

S-wave – parity violating (PV); P-wave – parity conserving (PC):

$$\Lambda\,(j^P = 1/2^+) \to p\,(j^P = 1/2^+)\,\pi^-(j^P = 0^-)$$

Measuring polarization – polarimetry in τ decays

[Tsai:1971vv, Kuhn:1991cc, Davier:1992nw, Kuhn:1995nn, Kuhn:1982di, Kuhn:1993ra, Hagiwara:1989fn]

Idea: similar relation for τ lepton decays,

$$\frac{\Phi}{\Gamma}\frac{\mathrm{d}\Gamma}{\mathrm{d}\Phi} \propto 1 + \vec{P}\cdot\vec{h}\,.$$

- $\vec{P}$ is a polarization of τ
- $\vec{h}$ is a **polarimeter vector**

Polarimeter vector of the τ lepton in the SM

- Direction depends on the final state, e.g.
  - for $\tau^- \to \pi^-\nu_\tau$ decay, $\vec{h} \uparrow\uparrow \vec{p}_{\pi^-}$
  - for $\tau^- \to \ell\nu_\tau\overline{\nu}_\ell$ decay, $\vec{h} \uparrow\uparrow \vec{p}_{\overline{\nu}_\ell}$
- Unit vector: $|\vec{h}| = 1$.

Measuring polarization – general multibody decays?

$\rightarrow$ Dalitz-Plot Decomposition (DPD)

Factorization of variables describing dynamics and polarization [JPAC:2019ufm]:

$$T_{\nu_0,\{\lambda\}}(\phi,\theta,\chi;\tau) = \sum_{\nu} D^{1/2}_{\nu_0,\nu}(\phi,\theta,\chi)\, A_{\nu,\{\lambda\}}(\tau)$$

Polarization d.o.f.

- Euler angles in active ZYZ convention
- rotation of the system as rigid body
- polarization affects angular distribution

Dynamic d.o.f.

- Mandelstam variables of the subsystems
- describes resonances in the decay

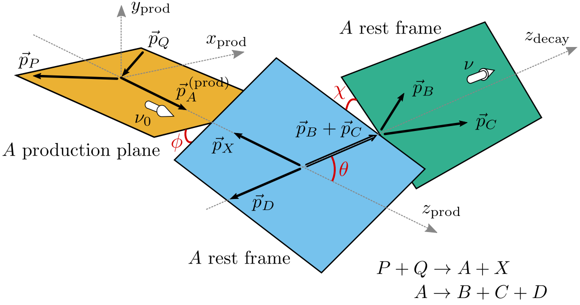

Dynamic d.o.f. for three-body decay

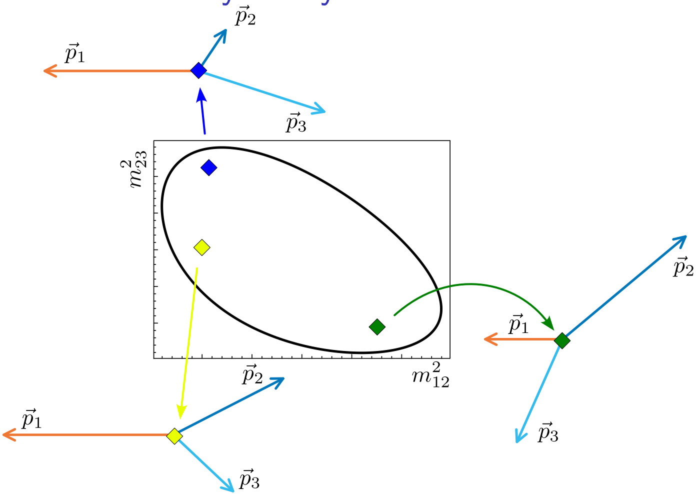

- For 3b decay: 2 degrees of freedom – Dalitz-plot coordinates
- (m_{12}^2, m_{23}^2) fixes orientation of the momenta

Model-agnostic representation of the decay rate

Using the SU(2) $\to$ SO(3) homomorphism, we get our polarized **master formula**,

$$|\mathcal{M}(\phi,\theta,\chi,\tau)|^2 = I_0(\tau)\left(1+\sum_{i,j=1}^{3} P_i R_{ij}(\phi,\theta,\chi)\alpha_j(\tau)\right),$$

where

- $I_0(\tau)$ is the unpolarized intensity
- $R(\phi,\theta,\chi) = R_Z(\phi)R_Y(\theta)R_Z(\chi)$ defines the decay plane orientation.
- $\alpha(\tau)$ is the **aligned polarimeter vector** field,

$$\vec{\alpha}(\tau) = \sum_{\nu',\nu,\{\lambda\}} A^*_{\nu',\{\lambda\}}\vec{\sigma}_{\nu',\nu}A_{\nu,\{\lambda\}} \Big/ I_0(\tau)\,.$$

It is specific for the decay, *does not depend on the production mechanism*.

Model-agnostic representation of the decay rate

Using the SU(2) $\to$ SO(3) homomorphism, we get our polarized **master formula**,

$$|\mathcal{M}(\phi,\theta,\chi,\tau)|^2 = I_0(\tau)\left(1+\sum_{i,j=1}^{3} P_i R_{ij}(\phi,\theta,\chi)\alpha_j(\tau)\right),$$

This study

where

- $I_0(\tau)$ is the unpolarized intensity
- $R(\phi,\theta,\chi) = R_Z(\phi)R_Y(\theta)R_Z(\chi)$ defines the decay plane orientation.
- $\alpha(\tau)$ is the **aligned polarimeter vector** field,

Determining polarization

1. provide $I_0(\tau)$ and $\vec{\alpha}(\tau)$
2. measure $|\mathcal{M}(\phi,\theta,\chi,\tau)|^2$
3. get $\vec{P}$ from fit

$$\vec{\alpha}(\tau) = \sum_{\nu',\nu,\{\lambda\}} A^*_{\nu',\{\lambda\}}\vec{\sigma}_{\nu',\nu}A_{\nu,\{\lambda\}} \Big/ I_0(\tau)\,.$$

It is specific for the decay, *does not depend on the production mechanism*.

Visualizing vector $\vec{\alpha}$

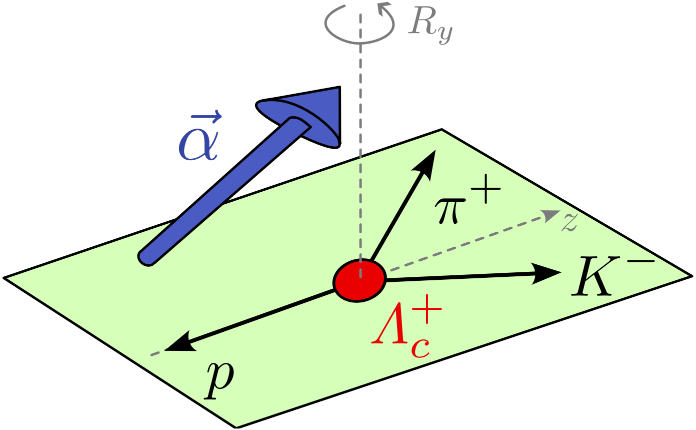

- $\vec{\alpha}$ is a vector with respect to the decay plane
- R_y is alignment rotation: who is z-axes (proton, kaon, or pion)
- numbering (p, π^+, K^-) vs (p, K^-, π^+) flips the plane

Aligned polarimeter vector field in Dalitz plot coordinates [LHCb:2023crj]

$$|\mathcal{M}(\phi,\theta,\chi,\tau)|^2 = I_0(\tau)\left(1+\sum_{i,j=1}^{3} P_i R_{ij}(\phi,\theta,\chi)\alpha_j(\tau)\right)$$

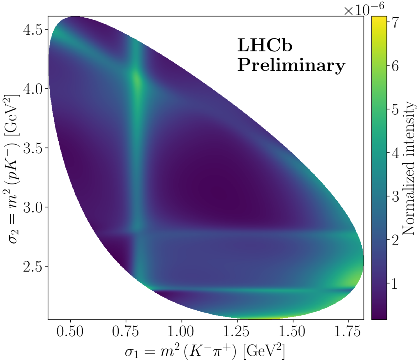

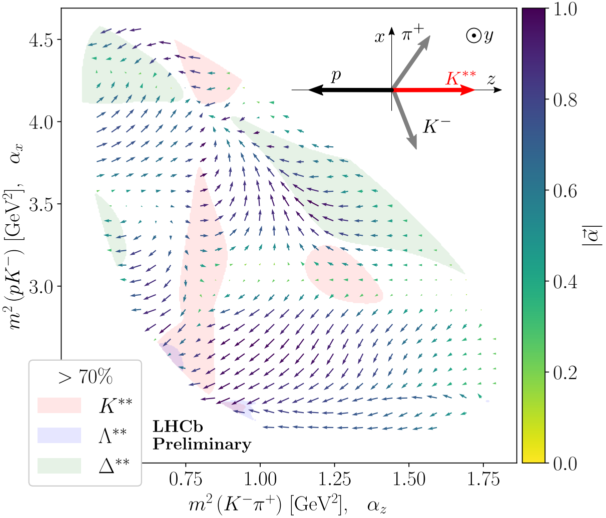

Summary on the excitation pattern

$1P$ multiplet of "bad" diquark – a fundamental piece of the baryon spectroscopy puzzle

- 7 states: five λ-modes and two ρ-modes
- In common for Ξ, $\Sigma_{b/c}$, $\Omega_{b/c}$, $\Xi_{b/c}$, Ξ_{cc}
- State splittings indicate spin-orbit and "hyperfine" interaction
- Charm (beauty) baryons are narrow – good chance to resolve it:
  - ! Assign quantum numbers, reveal the light quark dynamics
  - ! Identify diquark excitation for the first time

Summary on the excitation pattern

$1P$ multiplet of "bad" diquark – a fundamental piece of the baryon spectroscopy puzzle

- 7 states: five λ-modes and two ρ-modes
- In common for Ξ, $\Sigma_{b/c}$, $\Omega_{b/c}$, $\Xi_{b/c}$, Ξ_{cc}
- State splittings indicate spin-orbit and "hyperfine" interaction
- Charm (beauty) baryons are narrow – good chance to resolve it:
  - ! Assign quantum numbers, reveal the light quark dynamics
  - ! Identify diquark excitation for the first time

The threshold structure

- Is a state? (a partner of $D_s(2317)$) Compact / Molecular component?
- Present at other sectors?

The fifth narrow state

- Why only seen in inclusive $\Xi_c^+ K^-$
- The first manifestation of the diquark excitation? $2S$ states?

Summary on the excitation pattern

$1P$ multiplet of "bad" diquark – a fundamental piece of the baryon spectroscopy puzzle

- 7 states: five λ-modes and two ρ-modes
- In common for Ξ, $\Sigma_{b/c}$, $\Omega_{b/c}$, $\Xi_{b/c}$, Ξ_{cc}
- State splittings indicate spin-orbit and "hyperfine" interaction
- Charm (beauty) baryons are narrow – good chance to resolve it:
  - ! Assign quantum numbers, reveal the light quark dynamics
  - ! Identify diquark excitation for the first time

The threshold structure

- Is a state? (a partner of $D_s(2317)$) Compact / Molecular component?
- Present at other sectors?

The fifth narrow state

- Why only seen in inclusive $\Xi_c^+ K^-$
- The first manifestation of the diquark excitation? $2S$ states?

Powerful angular analysis will help resolving spin structure.

Prospects to utilize the charm-baryon polarimetry fields

- Mechanism of quark hadronization [Brambilla:2010cs, Faccioli:2010kd, Butenschoen:2012px]
- BSM searches with $\Lambda_b^0 \to \Lambda_c^+ \ell^- \nu$
  [Konig:1993wz, Dutta:2015ueb, Shivashankara:2015cta, Li:2016pdv, Li:2016pdv, Datta:2017aue, Ray:2018hrx, DiSalvo:2018ngq, Penalva:2019rgt, Ferrillo:2019owd]
  E.g. sign of longitudinal polarization of Λ_c^+ provides a test for left-handedness of $b \to c$ current
- BSM searches with measurement of EDM/MDM with charmed mesons
  [Baryshevsky:2016cul, Botella:2016ksl, Fomin:2017ltw]
- Hadron spectroscopy, extending decay chains
  - ✓ $\Lambda_b^0 \to J/\psi p K$ with $J/\psi \to \mu^+\mu^-$
  - ✓ $\mathfrak{B} \to J/\psi \bar{p} \Lambda$ with $\Lambda \to p\pi^-$
  - ? $\mathfrak{B}^+ \to \Lambda_c^+ \bar{\Lambda}_c^- K^+$ with $\Lambda_c^+ \to pK^-\pi^+$
  - ? $\Omega_b^- \to \Xi_c^+ \pi^- K^-$ with $\Xi_c^+ \to pK^-\pi^+$

[LHCb:2020gnv] Aaij *et al.*, "Observation of a New Excited D_s^+ Meson in $B^0 \to D^- D^+ K^+ \pi^-$ Decays," *Phys. Rev. Lett.*, vol. 126, no. 12, p. 122002, 2021, 10.1103/PhysRevLett.126.122002.

[LHCb:2018haf] Aaij *et al.*, "Observation of Two Resonances in the $\Lambda_b^0 \pi^\pm$ Systems and Precise Measurement of $\Sigma_b^\pm$ and $\Sigma_b^{*\pm}$ properties," *Phys. Rev. Lett.*, vol. 122, no. 1, p. 012001, 2019, 10.1103/PhysRevLett.122.012001.

[Belle:2017jrt] Li *et al.*, "Observation of $\Xi_c(2930)^0$ and updated measurement of $B^- \to K^- \Lambda_c^+ \bar{\Lambda}_c^-$ at Belle," *Eur. Phys. J. C*, vol. 78, no. 3, p. 252, 2018, 10.1140/epjc/s10052-018-5720-5.

[LHCb:2022vns] "Study of the $B^- \to \Lambda_c^+ \bar{\Lambda}_c^- K^-$ decay," 11 2022.

[Karliner:2017kfm] Karliner and Rosner, "Very narrow excited Ω_c baryons," *Phys. Rev. D*, vol. 95, no. 11, p. 114012, 2017, 10.1103/PhysRevD.95.114012.

[Padmanath:2017lng] Padmanath and Mathur, "Quantum Numbers of Recently Discovered Ω_c^0 Baryons from Lattice QCD," *Phys. Rev. Lett.*, vol. 119, no. 4, p. 042001, 2017, 10.1103/PhysRevLett.119.042001.

[Wang:2017zjw] Wang, "Analysis of $\Omega_c(3000)$, $\Omega_c(3050)$, $\Omega_c(3066)$, $\Omega_c(3090)$ and $\Omega_c(3119)$ with QCD sum rules," *Eur. Phys. J. C*, vol. 77, no. 5, p. 325, 2017, 10.1140/epjc/s10052-017-4895-5.

[LHCb:2017uwr] Aaij *et al.*, "Observation of five new narrow Ω_c^0 states decaying to $\Xi_c^+ K^-$," *Phys. Rev. Lett.*, vol. 118, no. 18, p. 182001, 2017, 10.1103/PhysRevLett.118.182001.

[Belle:2017ext] Yelton *et al.*, "Observation of Excited Ω_c Charmed Baryons in e^+e^- Collisions," *Phys. Rev. D*, vol. 97, no. 5, p. 051102, 2018, 10.1103/PhysRevD.97.051102.

[LHCb:2020tqd] Aaij *et al.*, "First observation of excited Ω_b^- states," *Phys. Rev. Lett.*, vol. 124, no. 8, p. 082002, 2020, 10.1103/PhysRevLett.124.082002.

[LHCb:2021ptx] Aaij *et al.*, "Observation of excited Ω_c^0 baryons in $\Omega_b^- \to \Xi_c^+ K^- \pi^-$ decays," *Phys. Rev. D*, vol. 104, no. 9, p. L091102, 2021, 10.1103/PhysRevD.104.L091102.

[Karliner:2023okv] Karliner and Rosner, "Excited Ω_c baryons as 2S states," 4 2023.

[LHCb:2023rtu] "Observation of new Ω_c^0 states decaying to the $\Xi_c^+ K^-$ final state," 2 2023.

[Tsai:1971vv] Tsai, "Decay correlations of heavy leptons in $e^+e^- \to \ell^+\ell^-$," *Phys. Rev. D*, vol. 4, no. 9, pp. 2821–2837, Nov. 1971, 10.1103/PhysRevD.4.2821.

[Kuhn:1991cc] Kühn and Mirkes, "Angular distributions in semileptonic τ decays," *Phys. Lett. B*, vol. 286, no. 3, pp. 381–386, Jul. 1992, 10.1016/0370-2693(92)91791-7.

[Davier:1992nw] Davier *et al.*, "The optimal method for the measurement of tau polarization," *Phys. Lett. B*, vol. 306, no. 3-4, pp. 411–417, Jun. 1993, 10.1016/0370-2693(93)90101-M.

[Kuhn:1995nn] Kühn, "τ polarimetry with multimeson states," *Phys. Rev. D*, vol. 52, no. 5, pp. 3128–3129, Sep. 1995, 10.1103/PhysRevD.52.3128.

[Kuhn:1982di] Kühn and Wagner, "Semileptonic decays of the τ lepton," *Nucl. Phys. B*, vol. 236, no. 1, pp. 16–34, Apr. 1984, 10.1016/0550-3213(84)90522-4.

[Kuhn:1993ra] Kühn, "Tau kinematics from impact parameters," *Phys. Lett. B*, vol. 313, no. 3, pp. 458–460, Sep. 1993, 10.1016/0370-2693(93)90019-E.

[Hagiwara:1989fn] Hagiwara *et al.*, "τ polarization measurements at LEP and SLC," *Phys. Lett. B*, vol. 235, no. 1, pp. 198–202, Jan. 1990, 10.1016/0370-2693(90)90120-U.

[JPAC:2019ufm] Mikhasenko *et al.*, "Dalitz-plot decomposition for three-body decays," *Phys. Rev. D*, vol. 101, no. 3, p. 034033, Feb. 2020, 10.1103/PhysRevD.101.034033.

[LHCb:2023crj] "Λ_c^+ polarimetry using the dominant hadronic mode," 1 2023.

[Brambilla:2010cs] Brambilla *et al.*, "Heavy Quarkonium: Progress, Puzzles, and Opportunities," *Eur. Phys. J. C*, vol. 71, p. 1534, 2011, 10.1140/epjc/s10052-010-1534-9.

[Faccioli:2010kd] Faccioli *et al.*, "Towards the experimental clarification of quarkonium polarization," *Eur. Phys. J. C*, vol. 69, no. 3, pp. 657–673, Oct. 2010, 10.1140/epjc/s10052-010-1420-5.

[Butenschoen:2012px] Butenschoen and Kniehl, "J/ψ polarization at the Tevatron and the LHC: Nonrelativistic-QCD Factorization at the Crossroads," *Phys. Rev. Lett.*, vol. 108, no. 17, p. 172002, Apr. 2012, 10.1103/PhysRevLett.108.172002.

[Konig:1993wz] Konig *et al.*, "Determination of the $b \to c$ handedness using nonleptonic Λ_c decays," *Phys. Rev. D*, vol. 49, no. 5, pp. 2363–2368, Mar. 1994, 10.1103/PhysRevD.49.2363.

[Dutta:2015ueb] Dutta, "$\Lambda_b \to (\Lambda_c, p)\tau\nu$ decays within standard model and beyond," *Phys. Rev. D*, vol. 93, no. 5, p. 054003, Mar. 2016, 10.1103/PhysRevD.93.054003.

[Shivashankara:2015cta] Shivashankara *et al.*, "$\Lambda_b \to \Lambda_c\tau\bar{\nu}_\tau$ decay in the standard model and with new physics," *Phys. Rev. D*, vol. 91, no. 11, p. 115003, Jun. 2015, 10.1103/PhysRevD.91.115003.

[Li:2016pdv] Li *et al.*, "$\Lambda_c \to \Lambda_c\tau\bar{\nu}_\tau$ decay in scalar and vector leptoquark scenarios," *JHEP*, vol. 02, p. 068, Feb. 2017, 10.1007/JHEP02(2017)068.

[Datta:2017aue] Datta *et al.*, "Phenomenology of $\Lambda_b \to \Lambda_c\tau\bar{\nu}_\tau$ using lattice QCD calculations," *JHEP*, vol. 2017, no. 8, p. 131, Aug. 2017, 10.1007/JHEP08(2017)131.

[Ray:2018hrx] Ray *et al.*, "Probing new physics in semileptonic Λ_b decays," *Phys. Rev. D*, vol. 99, no. 1, p. 015015, Jan. 2019, 10.1103/PhysRevD.99.015015.

[DiSalvo:2018ngq] Di Salvo *et al.*, "Detailed study of the $\Lambda_b \to \Lambda_c\tau\bar{n}u_\tau$ decay," *Int. J. Mod. Phys. A*, vol. 33, no. 29, p. 1850169, Oct. 2018, 10.1142/S0217751X18501695.

[Penalva:2019rgt] Penalva *et al.*, "Further tests of lepton flavour universality from the charged lepton energy distribution in $b \to c$ semileptonic decays: The case of $\Lambda_b \to \Lambda_c\ell\bar{\nu}\ell$," *Phys. Rev. D*, vol. 100, no. 11, p. 113007, Dec. 2019, 10.1103/PhysRevD.100.113007.

[Ferrillo:2019owd] Ferrillo *et al.*, "Probing effects of new physics in $\Lambda_b^0 \to \Lambda_c^+\mu^-\bar{\nu}_\mu$ decays," *JHEP*, vol. 2019, no. 12, p. 148, Dec. 2019, 10.1007/JHEP12(2019)148.

[Baryshevsky:2016cul] Baryshevsky, "The possibility to measure the magnetic moments of short-lived particles (charm and beauty baryons) at LHC and FCC energies using the phenomenon of spin rotation in crystals," *Phys. Lett. B*, vol. 757, pp. 426–429, 2016, 10.1016/j.physletb.2016.04.025.

[Botella:2016ksl] Botella *et al.*, "On the search for the electric dipole moment of strange and charm baryons at LHC," *Eur. Phys. J. C*, vol. 77, no. 3, p. 181, 2017, 10.1140/epjc/s10052-017-4679-y.

[Fomin:2017ltw] Fomin *et al.*, "Feasibility of measuring the magnetic dipole moments of the charm baryons at the LHC using bent crystals," *JHEP*, vol. 08, p. 120, 2017, 10.1007/JHEP08(2017)120.

[LHCb-PAPER-2022-002] LHCb Collaboration *et al.*, "Amplitude analysis of $\Lambda_c^+ \to pK^-\pi^+$ decays from semileptonic production," *Phys. Rev. D*, Aug. 2022, 10.48550/arXiv.2208.03262.

Appendix

Spin hypotheses testing

[LHCb:2021ptx]

- 2d Log Likelihood ratio as a test statistics $t_{J|J'} = \frac{1}{N}\sum_{i=1}^{N} \log\left(I_J(\cos\theta_i)/I'_J(\cos\theta_i)\right)$

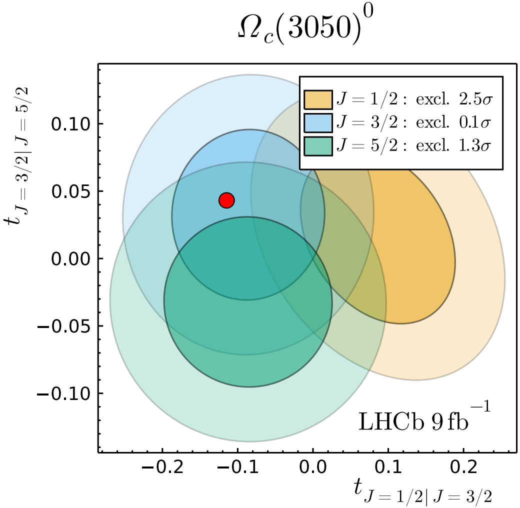

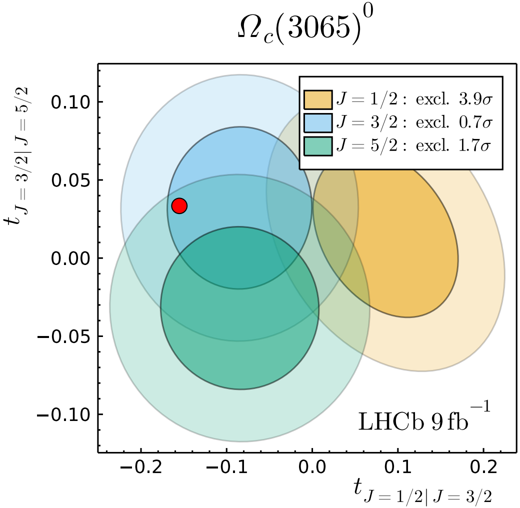

Optional simplification: averaging over dynamic variables

Can the dynamic variables τ be integrated over, i.e disregarded in the analysis?

$$\frac{8\pi}{\Gamma}\frac{\mathrm{d}^3\Gamma}{\mathrm{d}\phi\,\mathrm{d}\cos\theta\,\mathrm{d}\chi} = 1 + \sum_{i,j=1}^{3} P_i R_{ij}(\phi,\theta,\chi)\overline{\alpha}_j\,,$$

where $\vec{\overline{\alpha}}$ is **averaged aligned polarimeter vector**.

Advantage / Disadvantage

+ Only need know three numbers in order to determine polarization.
− Uncertainty on $\vec{P}$ with averaged $\vec{\overline{\alpha}}$ is worse than with the full $\vec{\alpha}(\tau)$ field. [Davier:1992nw]

Understanding the polarimeter vector

Example: $\Lambda_c^+ \to \Lambda(1520)\left(\to pK^-\right)\pi^+$

$\vec{\alpha}$ of individual contributions points in z-direction
when the resonance is aligned with z

Aligned

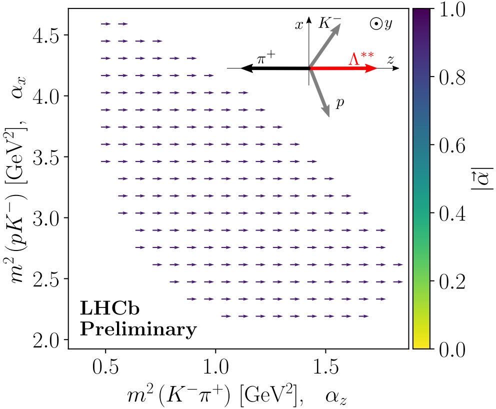

Misaligned

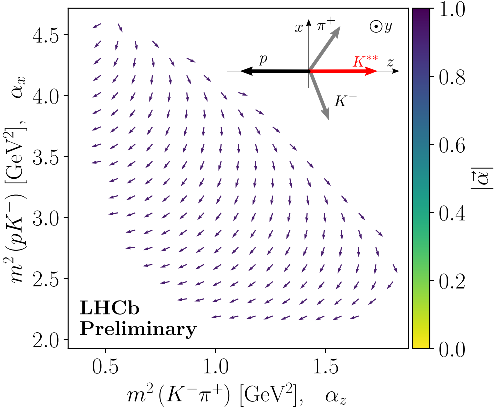

Polarization sensitivity by Davier et al.

Determination of polarization is a linear problem

$$I_0(\xi|P) = f(\xi) + Pg(\xi)\,, \quad \text{where } \xi \text{ are kinematic variables.}$$

For the likelihood fit of the set $\{\xi_i\}_N$, the error to P can be computed analytically:

$$P = P_{\mathrm{mod}} \pm \delta_P, \quad \delta_P = \frac{1}{S_P\sqrt{N}}, \text{ where } S_P^2 = \int \frac{g^2}{f+Pg} d^n\xi$$

Using the relations with our master formula

$$S_0 = 3 \int I_0\, |\vec{\alpha}|^2\, \mathrm{d}^n\tau \,/\, \int I_0\, \mathrm{d}^n\tau$$

- For integrated setup, $\overline{S}_0^2 = 3(\overline{\alpha}_x^2 + \overline{\alpha}_y^2 + \overline{\alpha}_z^2)$
- The ratio $S_0/\overline{S}_0$ gives the expected increase of the statistical uncertainty

Workflow and an input from amplitude analysis

- Implement $\Lambda_c^+ \to pK^-\pi^+$ models from [LHCb-PAPER-2022-002] with DPD
- Compute $\vec{\alpha}$ for every point of the $pK^-\pi^+$ Dalitz plot
- Propagate uncertainties of the angular analysis

[LHCb-PAPER-2022-002] provides:

- a default amplitude model
- several alternative models with different dynamics parametrizations
- parameter values with error bars for each model

Present project implemented:

- default model and alternative models formulated with DPD [JPAC:2019ufm]
- helicity couplings have been remapped
- guaranteed identical dynamics lineshapes

Implementation

Cross-check in two programming languages

This analysis has been performed in two languages:

`ThreeBodyDecay.jl`

symbolic amplitude models

Both implementations have been carefully documented on an interactive webpage

Next slides

A new technique: symbolic amplitude models

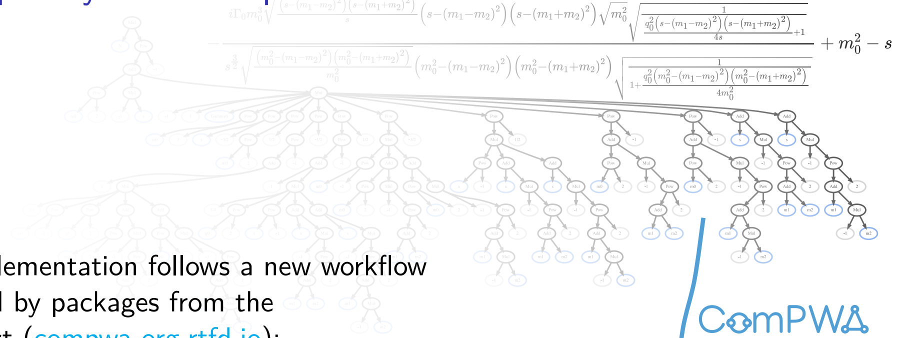

The Python implementation follows a new workflow that is facilitated by packages from the ComPWA Project (compwa-org.rtfd.io):

1. Formulate amplitude model **symbolically** with a Computer Algebra System
2. Use that symbolic expression as **template to a computational back-end**, such as a differentiable programming framework

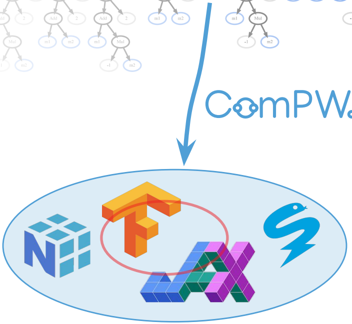

We selected **JAX** as the fastest back-end

A new technique: symbolic amplitude models

Advantages of this workflow:

- Computational implementation is **outsourced to fast, optimized back-ends** from the Machine Learning and data science community
- Out-of-the-box GPU and multi-threading support
- Very easy to implement other parametrizations without having to worry about performance
- CAS simplifications result in performance boosts
- Symbolic amplitude models result in a **self-documenting workflow**

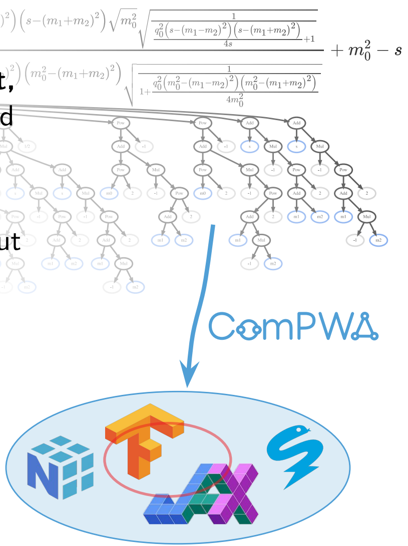

Works especially well for large computational models

Living documentation

Maintaining reproducible and understandable analysis results

Self-documenting workflow
Our analysis results are automatically rendered as static webpages from Jupyter and Pluto notebooks:
lc2pkpi-polarimetry.docs.cern.ch
(CERN SSO until on arXiv)

The Python and Julia dependencies are pinned, so that the analysis is **fully reproducible** in around 2 hours

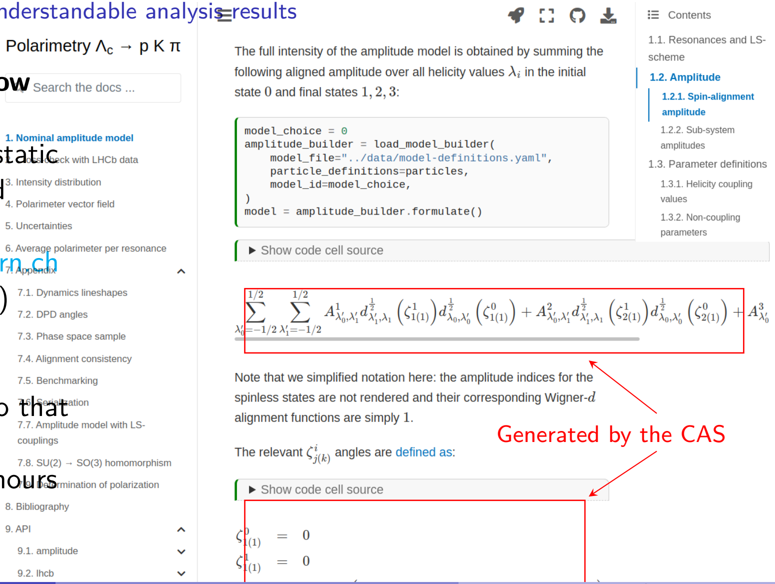

Generated by the CAS

Cross-checks

Visual comparison of the default amplitude model of [LHCb-PAPER-2022-002]

[LHCb-PAPER-2022-002]
(binned data)

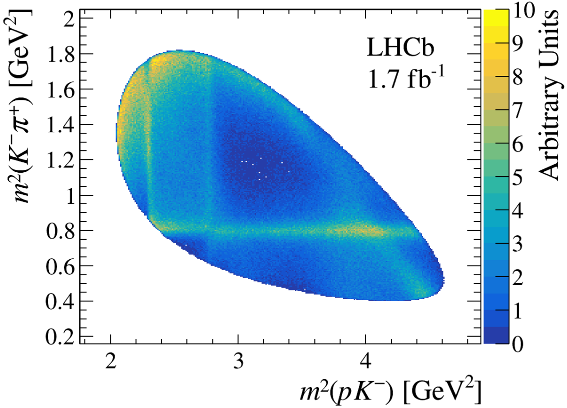

This analysis
(model evaluated on each Dalitz point)

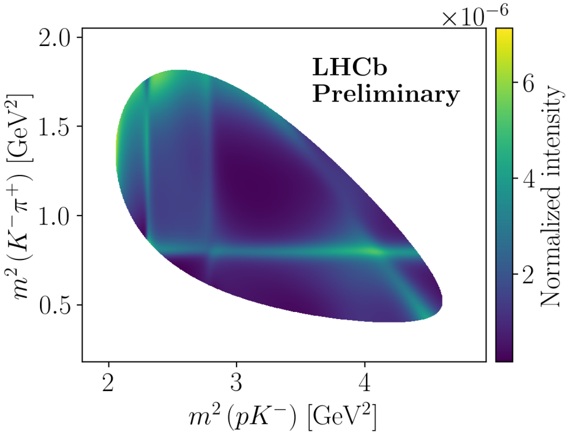

Cross-checks

Numerical test using code from LHCb-PAPER-2022-002

- Comparison for a single point in phase space
  - resonance lineshapes,
  - helicity amplitude per resonance
- Absolute differences at most 0.01%.

Search the docs ...

- Default amplitude model
- **Cross-check with LHCb data**
- Intensity distribution
- Polarimeter vector field
- Uncertainties
- Appendix
  - Dynamics lineshapes
  - DPD angles
  - Phase space sample
  - Alignment consistency
  - Benchmarking
  - Serialization

	Computed	Expected	Difference
`ArD(1232)1`	$\mathcal{H}^{\text{production}}_{D(1232),-\frac{1}{2},0}$		
`A++`	-0.488498+0.517710j	-0.488498+0.517710j	3.11e-14
`A+-`	0.894898-0.948412j	0.894898-0.948412j	7.61e-15
`A-+`	0.121490-0.128755j	0.121490-0.128755j	1.80e-14
`A--`	-0.222563+0.235872j	-0.222563+0.235872j	6.14e-15
`ArD(1232)2`	$\mathcal{H}^{\text{production}}_{D(1232),\frac{1}{2},0}$		
`A++`	-0.222563+0.235872j	-0.222563+0.235872j	6.14e-15
`A+-`	-0.121490+0.128755j	-0.121490+0.128755j	1.80e-14
`A-+`	-0.894898+0.948412j	-0.894898+0.948412j	7.61e-15

Contents

Propagation of uncertainties

Uncertainties over the polarimeter field have two components:

1. **Statistical + Systematic**:
   - parameter resampling of the default model using parameter error bars
   - parameter error bars include both stat. and syst. uncertainties, added in quadrature
   - take **RMS** over the resulting parameter-resampled distributions
2. **Model**:
   - determined from all alternative models
   - only central values of alternative models are considered
   - take **min-max** of the extrema

[LHCb-PAPER-2022-002, p. 19]

Table 8: Default amplitude model measured fit parameters describing the Λ contributions.

Parameter	Central Value	Stat. Unc.	Model Unc.	Syst. Unc.
$\mathrm{Re}\mathcal{H}^{\Lambda(1405)}_{1/2,0}$	-4.6	0.5	3.3	0.1
$\mathrm{Im}\mathcal{H}^{\Lambda(1405)}_{1/2,0}$	3.2	0.5	3.2	0.1
$\mathrm{Re}\mathcal{H}^{\Lambda(1405)}_{-1/2,0}$	10	1	12	0
$\mathrm{Im}\mathcal{H}^{\Lambda(1405)}_{-1/2,0}$	2.8	1.1	3.7	0.3
$\mathrm{Re}\mathcal{H}^{\Lambda(1520)}_{1/2,0}$	0.29	0.05	0.12	0.01
$\mathrm{Im}\mathcal{H}^{\Lambda(1520)}_{1/2,0}$	0.04	0.05	0.12	0.02
$\mathrm{Re}\mathcal{H}^{\Lambda(1520)}_{-1/2,0}$	-0.16	0.14	0.69	0.03
$\mathrm{Im}\mathcal{H}^{\Lambda(1520)}_{-1/2,0}$	1.5	0.1	1.3	0.0
$m^{\Lambda(1520)}$ [MeV]	1518.47	0.36	0.65	0.03
$\Gamma^{\Lambda(1520)}$ [MeV]	15.2	0.8	1.3	0.1
$\mathrm{Re}\mathcal{H}^{\Lambda(1600)}_{1/2,0}$	4.8	0.5	5.0	0.1
$\mathrm{Im}\mathcal{H}^{\Lambda(1600)}_{1/2,0}$	3.1	0.5	3.7	0.1
$\mathrm{Re}\mathcal{H}^{\Lambda(1600)}_{-1/2,0}$	-7.0	0.5	8.7	0.1
$\mathrm{Im}\mathcal{H}^{\Lambda(1600)}_{-1/2,0}$	0.8	0.6	2.0	0.2
$\mathrm{Re}\mathcal{H}^{\Lambda(1670)}_{1/2,0}$	-0.34	0.05	0.35	0.01
$\mathrm{Im}\mathcal{H}^{\Lambda(1670)}_{1/2,0}$	-0.14	0.05	0.22	0.02
$\mathrm{Re}\mathcal{H}^{\Lambda(1670)}_{-1/2,0}$	-0.57	0.10	0.46	0.02
$\mathrm{Im}\mathcal{H}^{\Lambda(1670)}_{-1/2,0}$	1.0	0.1	1.2	0.0
$\mathrm{Re}\mathcal{H}^{\Lambda(1690)}_{1/2,0}$	-0.39	0.10	0.23	0.02

Propagated uncertainties on the polarimeter field

We compute $\vec{\alpha}^{(i)}(\tau)$ over a phase space sample, with i one of the parameter resamplings or one of the alterative amplitude models.

Uncertainties are then visualized separately, using

- **vector norm**: $\left|\vec{\alpha}^{(i)} - \vec{\alpha}^{\text{default}}\right|$
- **solid angle**:

$$\delta\Omega^{(i)} = \int_0^{2\pi}\int_0^{\theta} \mathrm{d}\phi\,\mathrm{d}\cos\theta = 2\pi\left(1 - \cos\theta^{(i)}\right)$$

with $\cos\theta^{(i)} = \frac{\vec{\alpha}^{(i)}\cdot\vec{\alpha}^{\text{default}}}{|\vec{\alpha}^{(i)}||\vec{\alpha}^{\text{default}}|}$.

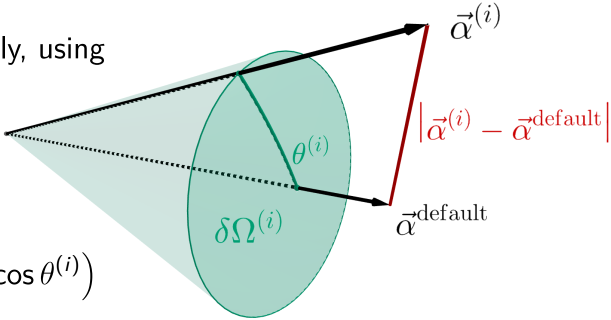

Propagated uncertainties on the polarimeter field

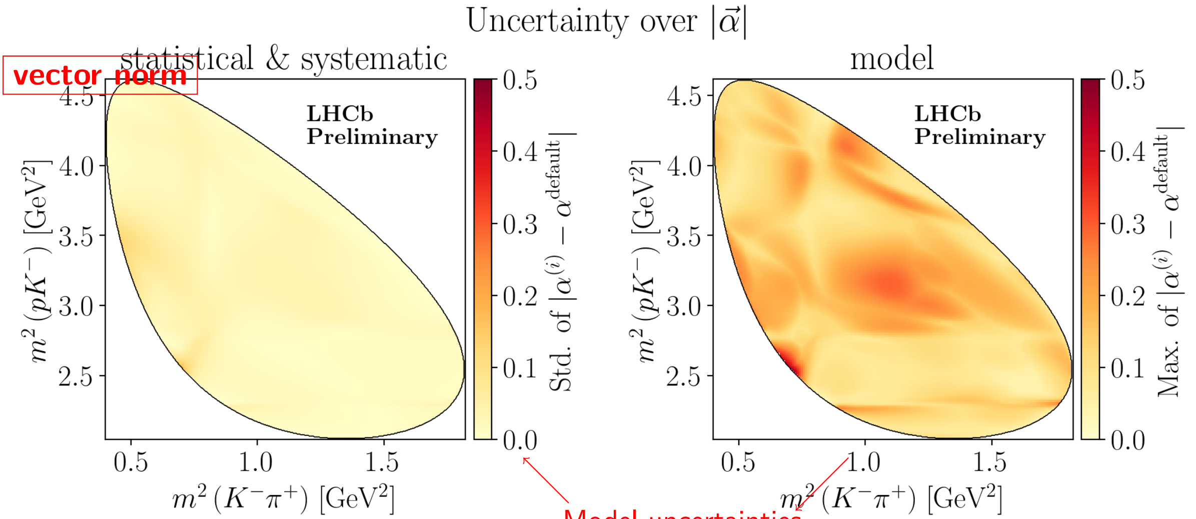

Model uncertainties
dominate over stat.&syst.

Propagated uncertainties on the polarimeter field

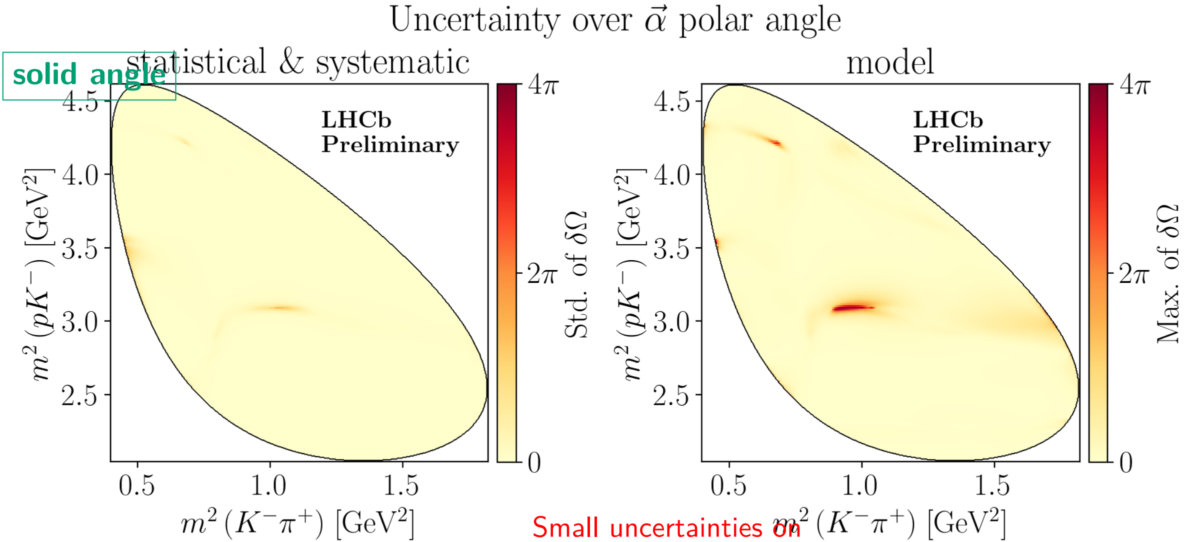

Small uncertainties on vector field directions

Averaged polarimeter vector

Defining the averaged polarimeter vector as $\overline{\alpha}_j = \int I_0 \alpha_j \mathrm{d}^n\tau \;/\; \int I_0 \, \mathrm{d}^n\tau$, we get:

$$
\begin{aligned}
\overline{\alpha_x} &= \left(-62.6 \pm 4.5^{+8.4}_{-14.8}\right) \times 10^{-3}\,, \\
\overline{\alpha_y} &= \left(+8.9 \pm 8.9^{+9.1}_{-12.7}\right) \times 10^{-3}\,, \quad \textcolor{red}{\text{(due to interference)}} \\
\overline{\alpha_z} &= \left(-278.0 \pm 23.7^{+12.6}_{-40.4}\right) \times 10^{-3}\,, \\
\overline{|\alpha|} &= \left(669.4 \pm 9.3^{+15.3}_{-10.4}\right) \times 10^{-3}\,. \quad \textcolor{red}{(\approx |\overline{\alpha}| \times 2.35)}
\end{aligned}
$$

First uncertainty is stat.&syst (std.), second is model (extrema of alternative models).

Averaged polarimeter vector

Defining the averaged polarimeter vector as $\overline{\alpha}_j = \int I_0 \alpha_j \mathrm{d}^n\tau \,/\, \int I_0 \, \mathrm{d}^n\tau$, we get:

$$\begin{aligned}
\overline{\alpha_x} &= \left(-62.6 \pm 4.5^{+8.4}_{-14.8}\right) \times 10^{-3}\,, \\
\overline{\alpha_y} &= \left(+8.9 \pm 8.9^{+9.1}_{-12.7}\right) \times 10^{-3}\,, \quad \text{(due to interference)} \\
\overline{\alpha_z} &= \left(-278.0 \pm 23.7^{+12.6}_{-40.4}\right) \times 10^{-3}\,, \\
\overline{|\alpha|} &= \left(669.4 \pm 9.3^{+15.3}_{-10.4}\right) \times 10^{-3}\,. \quad (\approx |\overline{\alpha}| \times 2.35)
\end{aligned}$$

First uncertainty is stat.&syst (std.), second is model (extrema of alternative models).

Spherical coordinates (less correlated resampling uncertainty):

$$\begin{aligned}
|\overline{\alpha}| &= \left(+285.1 \pm 24.0^{+37.9}_{-13.8}\right) \times 10^{-3}\,, \\
\theta\left(\overline{\alpha}\right) &= \left(+0.929 \pm 0.002^{+0.017}_{-0.011}\right) \times \pi\,, \quad \text{(small error!)} \\
\phi\left(\overline{\alpha}\right) &= \left(+0.955 \pm 0.045^{+0.067}_{-0.028}\right) \times \pi\,.
\end{aligned}$$

Results availability

Justification of the 100x100 grid

Numeric

$\vec{\alpha}(\tau)$ and $I_0(\tau)$ available in grid form:

- For propagating uncertainties:
  - grids for default model, all alternative models, and resampled
- Grid size in $\delta m_{pK} \sim \Gamma_{\Lambda(1520)}$
- Toy fits of $\vec{P}$ with grids of **100x100**, 200x200, 500x500 $\Rightarrow$ negligible extra uncertainty

lc2pkpi-polarimetry.docs.cern.ch

averaged-polarimeter-vectors.json (33.7 kB)

polarimetry-field.json (67.9 MB)

polarimetry-field.tar.gz (26.2 MB)

Symbolic

The symbolic model is easy picklable:

```python
import pickle
import jax.numpy as jnp

# COMPWA
from tensorwaves.function.sympy import create_function

# load model
model_description = pickle.load("Lc2pKpi-sympy-default-model.pkl")

# substitute parameters
sympy_model = (model_description["intensity_expr"]
    .xreplace(model_description["parameter_defaults"]))

# compile < 1s
density = create_function(sympy_model, backend="jax")

# call
density({"sigma1": jnp.array([1.0, 1.1]), "sigma2": jnp.array([3.0, 3.2])})
```